Developing a Three- to Six-State EEG-Based Brain–Computer Interface for a Virtual Robotic Manipulator Control

Yuriy Mishchenko, Murat Kaya, Erkan Ozbay, and Hilmi Yanar

Abstract*—*Objective: **We develop an electroencephalography (EEG)-based noninvasive brain–computer interface (BCI) system having short training time (15 min) that can be applied for high-performance control of robotic prosthetic systems.** ***Methods:*** **A signal processing system for detecting user's mental intent from EEG data based on up to six-state BCI paradigm is developed and used.** ***Results:*** **We examine the performance of the developed system on experimental data collected from 12 healthy participants and analyzed offline. Out of 12 participants 3 achieve an accuracy of six-state communication in 80%–90% range, while 2 participants do not achieve a satisfactory accuracy. We further implement an online BCI system for control of a virtual 3 degree-of-freedom (dof) prosthetic manipulator and test it with our three best participants. Two participants are able to successfully complete 100% of the test tasks, demonstrating on average the accuracy rate of 80% and requiring 5–10 s to execute a manipulator move. One participant failed to demonstrate a satisfactory performance in online trials.** ***Conclusion:*** **We show that our offline EEG BCI system can correctly identify different motor imageries in EEG data with high accuracy and our online BCI system can be used for control of a virtual 3 dof prosthetic manipulator.** ***Significance:*** **Our results prepare foundation for further development of higher performance EEG BCI-based robotic assistive systems and demonstrate that EEG-based BCI may be feasible for robotic control by paralyzed and immobilized individuals.**

***Index Terms*—Brain machine interfaces, electroencephalography, neural prosthetics.**

I. Introduction

INVASIVE/NONINVASIVE brain–computer interfaces (BCI) that directly translate neural activity in the cortex into a control signal for external devices provide improved communication and control for paralyzed patients [1], [2]. Recent advances in invasive BCI research including neural control of robotic manipulators realized in nonhuman primates and virtual 2D/3D control by paralyzed individuals demonstrated that invasive BCI have provided important achievements for control of robotic prosthetic technology with a high degree of efficiency and accuracy [3]–[10]**.** Despite these impressive achievements, intracranial BCI represent significant risks to their users associated with the necessarily of invasive brain surgery. Thus, exploring the potential for a high-performance control of brain-computer interfacing technologies using only noninvasive brain activity imaging means is of great interest.

Information about users' motor intent has been shown in the literature to exist in cortical activity in a variety of frequency bands and spatial scales from local field potentials (LFP), to electrocorticography (ECoG), functional Magnetic Resonance Imaging (fMRI), magnetoencephalography (MEG) and electroencephalography (EEG) scales [11]. In that relation, EEG represents a point of special interest given the ease with which EEG data can be acquired, the maturity of the technology, the portability, versatility and relatively low cost of modern EEG acquisition devices as contrasted with invasive and other noninvasive brain activity imaging techniques. Therefore, EEG based BCIs have begun to be widely used. EEG-based BCIs have been used for control of both 2D/3D virtual objects [12]–[16] and real objects such as robotic manipulators, quadcopter and wheelchairs [17]–[19].

In EEG-BCI technology, it is well known that long training times of BCI decoder and subjects is a significant disadvantage. If long training times can be reduced without causing significant loss in performance of the EEG based BCIs, more efficient EEG-BCIs could be developed. Recently, in EEG-BCI field, some studies showed that the control of 2D/3D virtual and real objects have been achieved successfully using short training ($\sim$20 min) session [12], [18]. In this context we have aimed to develop a more efficient noninvasive EEG-based BCI system requiring only a 15-minute training session that can be applied in the future towards a high performance control of a robotic manipulator envisioned as a part of an assistive robotic complex for paralyzed or immobilized patients.

The paper is organized as follows. Section II describes the process of EEG data collection, pre-processing, and analysis both for our offline and online BCI applications. In Section III,

Manuscript received April 23, 2018; revised July 20, 2018; accepted August 10, 2018. Date of publication August 17, 2018; date of current version March 19, 2019. This work was supported in part by the TUBITAK ARDEB under Grant 113E611 and in part by the Young Investigator Award of the Science Academy under the BAGEP program. *(Corresponding author: Hilmi Yanar.)*

Y. Mishchenko is with the Biomedical Engineering Department, Izmir University of Economics.

M. Kaya is with the Computer Engineering Department, Mersin University.

E. Ozbay is with the Biophysics Department, Mersin University.

H. Yanar is with the Physics Department, Mersin University, Mersin 33110, Turkey (e-mail: hilmiyanar@mersin.edu.tr).

This paper has supplementary downloadable material available at http://ieeexplore.ieee.org.

Digital Object Identifier 10.1109/TBME.2018.2865941

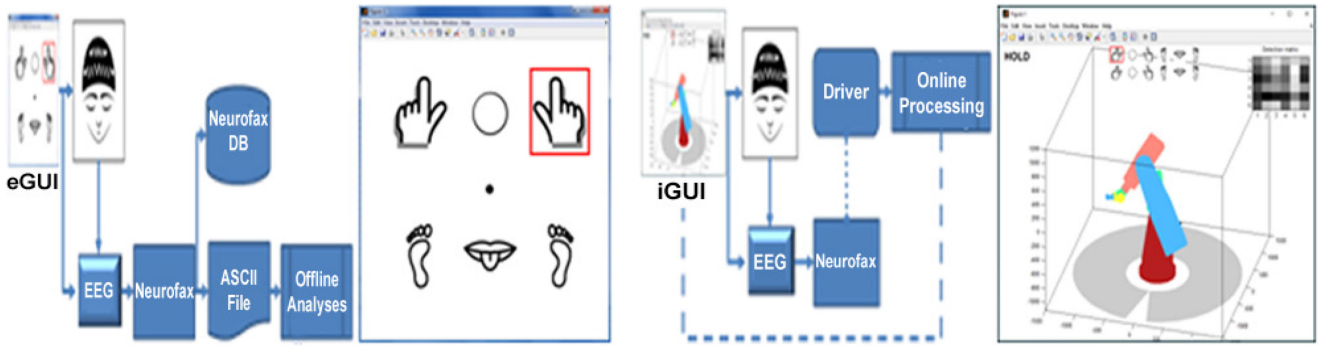

Fig. 1. (Left) Schematic representation of the offline experiments' procedure with experimental graphical user interface (eGUI). First, action signals had been presented to participants by indicating one of the motor imagery icons using a red rectangle on computer screen. The EEG signal in response to the implementation of shown motor imagery was acquired by EEG-1200 system and recorded using Neurofax software. After the completion of the experiment, the recorded EEG data was saved to Neurofax database as well as exported to an ASCII file for further custom offline processing. The graphical user interface used in offline experiment consisting of a single Matlab figure with 5 icons representing left hand, right hand, left leg, right leg, and tongue motor imageries, a passive signal indicated with a circle, a fixation point in the center, and an action signal shown as a red rectangle around right hand motor imagery icons. (Right) Schematic representation of the online experiments' procedure with interactive graphical user interface (iGUI). The participants attempted to control in real time a 3 dof robotic manipulator arm using the EEG BCI by implementing different motor imageries. The row EEG signal associated with implementation of each imagery was recorded by EEG-1200 system and imported to Matlab via custom memory-scanning driver software. The EEG data was then processed in a Matlab application and used to provide control signal for the robot arm. The online experiment's interactive graphical user interface (iGUI) consisting of a Matlab figure modeling in 3D the motion of a robot manipulator arm.

the ability of the developed system to discriminate different mental imagery states is examined on 12 participants using offline analysis of collected EEG data. Certain design choices of the BCI's data processing system including that of EEG data representation, detector window optimization, reference voltage choice, frequency filter, etc. are investigated. The results of interactive application of BCI for online control of a 3D robotic arm simulated on a computer screen by 3 participants are also presented. In Section IV, we discuss achieved results and compare them with the literature. Achieved performance and venues for potential improvement as well as the perspectives of the BCI's utilization in assistive robotic settings are discussed. Conclusions are offered in Section V.

II. Materials and Methods

A. Participants

Twelve volunteers including three (3) female and nine (9) male participated in this study after giving written informed consent. All participants were healthy and right-handed individuals. The average age of the female volunteers was 24.3 and the average age of the male volunteers was 28.5. Volunteers are selected among the students of the Faculty of Engineering at Toros University and the Department of Physics and the Department of Biophysics at Mersin University, Mersin, Turkey. All participants took orientation session informing them about the experiments' purpose, procedures, and their rights with respect to the collected information. All experimental procedures of the study had been reviewed and approved by the ethics committees of Toros University and Mersin University, Mersin, Turkey.

B. Data Acquisition and Experimental Procedures

The EEG data have been acquired using the medical grade EEG-1200 EEG recording system with JE-921A acquisition box (Nihon Kohden, Japan). In all experiments, a standard EEG cap (Electro-Cap International, USA) with 19 electrodes in the standard international 10–20 system (see Supplementary Materials Figure S1) and Electro-gel (Electro-Gel, Elector-Cap International, USA; Elefix Paste for EEG Z-401CE, Nihon Kohden, USA) have been used.

The participants have been comfortably seated in a recliner chair and then the EEG cap has been carefully placed onto participant's scalp. The electrodes have been filled with electro-gel. At the same time, the electrode impedances in the impedance-check mode of EEG 1200 Neurofax have been controlled and the impedances have been kept at or below 10 kOhm with the impedance imbalance at or below 5 kOhm. Once the EEG recordings preparation has been completed, the computer screen of the original base computer part of the EEG 1200 system has been positioned approximately 200 cm in front of the participants at slightly above the eye level.

The EEG experiments have been conducted in two formats–offline format and online format.

1) Offline Experiment Format: In the offline experiments, participants were asked to perform different motor imageries showed by the experiment's graphical user interface (eGUI) consisting of a Matlab figure with 5 icons encoding different motor imageries (left hand, right hand, left leg, right leg, tongue) as well as a "passive" icon represented by a circle and a gaze-fixation point in the center of the figure, see Fig. 1 (Left). Prior to the beginning of the data acquisition, the participants were instructed to remain motionless and keep their gaze fixed at the fixation point at all times during the experiment.

Offline experiments began with a 2.5-minute relaxation period, after which three 15-minute sessions followed separated by 2 minute breaks, for a total duration of approximately 1 hour, see Fig. 2. During each session, participants performed approximately 300 BCI trials each consisting of one 1-second visual

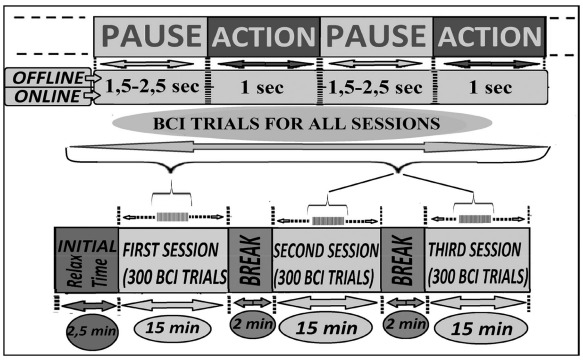

Fig. 2. Timeline for the offline and online experiments.

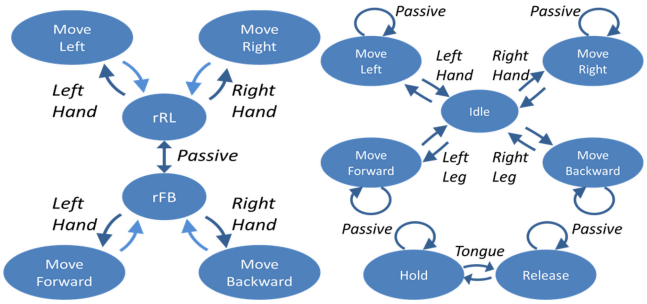

Fig. 3. (Left) Schematic representation of the 3-state BCI control model. Left and right hand movements are used to move the manipulator either left and right or back and forth depending on motion regime switched by passive imagery implementation. (Right) Schematic representation of the 6-state BCI control model. Each motor imagery initiates one type of motion of the robot arm that continues through passive imagery presentation until a second presentation of the same or a new presentation of another motor imagery.

action signal presentation that selected a motor imagery to be implemented by means of a red rectangle shown around the corresponding imagery's icon in eGUI, Fig. 1 (Left). The motor imageries were selected randomly following a pseudorandom sequence generated in the beginning of the experiment using a random number generator. The participants were instructed to implement the shown imagery for one time during the action period of 1 s in which the selection frame was visible.

A "passive" action signal was shown using a circle icon. During the passive signal, the participants were instructed to remain passive and to not intentionally respond in any way. A pause of duration varying from 1.5 to 2.5 seconds followed the presentation of each action signal, thus concluding the trial. In the during pause period of 1.5–2.5 s, the participants were remained motionless as they did during the passive signal. Each trial took on average 3 seconds to complete, Fig. 2.

The EEG signals from 19 EEG electrodes plus two A1–A2 ground electrodes were recorded during the entire duration of the experiment using Neurofax software (Nihon Kohden, Japan). The recording settings used were the sampling rate of 200 Hz, the low frequency cut-off of 0.53 Hz, and the high frequency cut off 70 Hz. A custom montage including all the electrodes with system 0 Volt-reference was created in Neurofax and used in the recordings, archived data, ASCII exported data and imported to Matlab (convert_nkascii2mat.m function by Timothy Ellmore available from Beauchamp at OpenWetWare.org).

2) Online Experiment Format: The preparation of experiments and the recording of EEG signals were performed in the same way as described for the offline experiments. In order to acquire the EEG data from EEG-1200 in real time, we have developed a custom driver software using C#. The extracted data was then forwarded to our main BCI application in Matlab.

In the online experiments, the participants were asked to control a 3 dof robot manipulator arm simulated on a computer screen in 3D, using our EEG BCI, Fig. 1 (Right). The robot manipulator could perform left-right, forward-backward, and hold-release motions, controlled by up to 6 mental imageries including left and right hand movement, left and right leg movement, tongue movement, and one passive imagery.

The online experiments followed a protocol essentially similar to that used in the offline experiments. Namely, the online experiments were structured as three 15-minutes sessions separated by 2-minute breaks, with a 2.5-minute initial relaxation period, Fig. 2. The first 15-minute session was used to train the BCI decoder. The organization of the training session was essentially similar to that of the offline experiments described in Section II-B1. The second 15-minute session was used as a practice session. During that time, the participants used the previously trained BCI to try and assume the control of the manipulator arm in a free exploration manner by implementing the imagery of their choice in voluntary manner. The third 15-minute session was used as a test session. During that time, the participants were given instructions to execute a set of simple tasks by using the robot arm and the BCI. The tasks consisted of moving the robot arm to a specified location such as "move robot arm two steps to the left" or "move robot arm two steps to the left and two steps forward". The participants allowed to spontaneously control the robotic device using his\her own strategy to all tasks.

3) BCI Control Models: In this work, two BCI control models were employed, a 3-state control model and a 6-state control model. In the 3-state control model, only left-right hand and passive imageries were used. Left and right hand movement imageries were used to move the manipulator either left and right or back and forth, depending on the regime that could be switched among by the user using the passive imagery, left panel in Fig. 3. For example, a user could move the manipulator left or right by implementing left or right hand movements first, then, in order to move the manipulator forward or backward, the user could stay passive for one round during which the BCI would switch from left-right to forward-backward motion regime, and then continue using the left or right hand movements to move the manipulator forward or backward, respectively. In order to switch the regime back, the user again could remain passive for one period. The observation of hand movement imageries moved the robot one step in the corresponding direction. Therefore, continuously moving the robot arm required the user to implement the desired imagery continuously over a sequence of "on"-signal presentation periods.

In the 6-state control model, each of the five distinct motor imageries and one passive state were used as a control signal

for the simulated robot arm. Each motor imagery was bound to one type of motion of the robot arm: Left and right hand movement imageries were bound to the motion of robot arm in left and right direction; leg movement imageries were bound to the forward and backward motion of the robot arm, tongue movement imagery was bound to the arm's grabber hold or release motion, right panel in Fig. 3. The passive state was used to continue a previously started movement. Each motor imagery was used to initiate one motion in corresponding direction, and the motion continued until a second presentation of the same imagery or a presentation of a different motor imagery was encountered. The second observation of the same motor imagery stopped the motion of the robot arm while the observation of a different motor imagery stopped the current motion and initiated the new motion of the arm.

C. Offline Data Analysis

The analysis of collected EEG data in the offline experiments was performed offline after the conclusion of each experiment. For that, the EEG data was first exported from Neurofax software into an ASCII file and imported to Matlab using a custom script, as described in the previous section. The EEG data thus imported to Matlab was a matrix of EEG voltage readings, E_{it}, where $t = 1, \ldots, T$ indexed the different time samples and $i = 1, \ldots, N_e$ indexed the EEG channels. A total of $N_e = 22$ data channels were imported, with 19 channels corresponding to the EEG electrodes in the standard 10–20 configuration, two channels describing the A1–A2 electrodes, and the 22nd channel encoding the eGUI synchronization-signal on the X3 bipolar input. The raw EEG data was collected in system 0 Volt-reference (defined by EEG-1200 manual as the average of the voltage values on C3 and C4 electrodes) and then digitally re-referenced to a given voltage reference. For different analyses described below in Section III-B, we considered the system 0V-reference (defined above), the average A1–A2 reference (defined as the average of the A1 and A2 voltages), the common average reference (defined as the average of all electrodes' voltages), and the Laplace reference (defined as the average of the voltages on each electrode's 4 immediate neighbors). The data in the 22nd sync-channel was used to establish the onset times of the action and to bind each action signal in eGUI to a specific onset time. Other than re-referencing and binding of the action signals, no other preprocessing was performed on raw EEG data.

The EEG data was partitioned into data frames corresponding to different presentations of action signal for further processing, by selecting the fragments of EEG data within $[t_1, t_2]$-data frames locked to the action signal onset time. The stack of such data frames could be represented as a 3-dimensional array, E_{nit}, with the indexes i and t having the same meaning as before (except that t changed from 1 to $dt = t_2 - t_1$ - the length of the frame), and the index n enumerating different trials or action signal presentation episodes. Generally, the first second of EEG data immediately following the onset of the action signal could be used as the data frames for decoding, which coincided with the time during which the action signal was on and the participants carried out mental imageries. However, we further optimized the data-frame selection by considering all possibilities for the frame onset, $t_1 \in [-0.5, 1.0]$ sec, and end-time, $t_2 \in [0.0, 2.0]$ sec, at 0.1 second intervals. As described in Results, the decoding data frame choice of $t_1 = 0$ sec and $t_2 = 0.85$ sec was found to offer the best overall performance for all subjects and all mental imageries.

After partitioning the EEG recording into data frames, the decoder for associating data frames with mental imageries was constructed using SVM or LDA machine learning algorithms. For that, first, the EEG data from each frame was converted into a feature-vector representation. We experimented with several feature representations of EEG signal including Power Spectral Density (PSD), EEG band power (EEG band), Fourier transform amplitudes (FTA), and raw time series (TS). Information on how the features are specifically defined and calculated has been given in the supplementary material.

After calculating the feature vectors for each trial, SVM and LDA machine learning algorithms were used to build decoders classifying each data frame as a specific mental imagery. LDA and SVM both have been used widely and enjoyed a significant success in EEG BCI and we do not go further into the details of these established algorithms here, whereas extensive literature is available on the subject for interested reader, see [20] and references therein.

The classifiers were trained and their performance was evaluated using the cross-validation method, standard in the machine learning literature, using either randomized and sequential hold-out cross-validation with 70% of data used for training and 30% used for validation purposes.

D. Online Data Processing

For interactive BCI control, we implemented the EEG data analysis system and an interactive real-time BCI application using Matlab. The interactive graphical user interface (iGUI) that we developed acquired raw EEG data from EEG-1200 in real time and performed learning of the BCI decoder as well as applied such decoder to offer a real-time control of a 3D robot manipulator arm simulated in on computer screen as shown in Fig. 1.

During the training sessions of the online experiments, the mentioned application collected a certain number of EEG data frames exemplifying different user's motor imageries, as instructed by a pseudorandom training program. Typically, 300 motor imagery examples were collected during the training session and thus used to build the EEG BCI signal decoder, as described above. The data frame selection of [0, 0.85] sec, FTA features in Cartesian form, and multi-class SVM were used for such a final decoder. After the training session, during the practice and the test sessions, the EEG data was acquired, data frames were selected and processed by the decoder online, in order to estimate the motor imagery class in real time and carry out the robot arm's movement guided by the EEG signal according to a specific BCI control model described above in Section II-B3. No artifact rejection was performed understanding that learning to ignore artifacts should be one of the goals of the decoder's classifier.

TABLE I
PARTICIPANTS PERFORMANCE IN 2-STATE BCI DISCRIMINATION TASK

Participant	Performance SVM				Performance LDA				Number of Exp.
	Average	STD	Worst	Best	Average	STD	Worst	Best	
ES	0.99	0,01	0.98	0.99	0.98	0.02	0.97	0.99	2
HI	0.98	0,01	0.96	0.99	0.94	0.04	0.88	0.98	5
YL	0.98	0,01	0.98	0.98	0.97	0.01	0.96	0.97	2
EM	0.96	0,04	0.93	1.00	0.95	0.03	0.92	0.97	3
SE	0.95	0.05	0.89	1.00	0.92	0.07	0.82	0.98	5
ER	0.95	0.06	0.89	0.99	0.94	0.06	0.88	0.97	3
YU	0.91	0.07	0.78	0.93	0.84	0.09	0.72	0.92	5
MR	0.88	0.08	0.74	0.92	0.79	0.06	0.73	0.86	5
EK	0.84	0.09	0.76	0.93	0.85	0.06	0.79	0.90	2
UL	0.81	0.05	0.76	0.87	0.79	0.05	0.74	0.84	2
BA	0.77	0.02	0.75	0.79	0.73	0.04	0.69	0.77	2
ME	0.75	0.12	0.66	0.84	0.70	0.07	0.62	0.77	2
Overall	0.90	0.09	0.66	1.00	0.87	0.1	0.62	0.99	38

TABLE II
PARTICIPANTS PERFORMANCE IN 3-STATE BCI DISCRIMINATION TASK

Participant	Performance SVM				Performance LDA			
	Average	STD	Worst	Best	Average	STD	Worst	Best
ES	0.98	0.02	0.96	0.99	0.97	0.01	0.95	0.97
YL	0.90	0.01	0.89	0.91	0.88	0.01	0.87	0.88
HI	0.89	0.04	0.86	0.95	0.90	0.04	0.85	0.95
ER	0.89	0.06	0.83	0.93	0.84	0.09	0.74	0.89
EM	0.85	0.05	0.80	0.89	0.82	0.12	0.81	0.83
SE	0.82	0.12	0.63	0.90	0.78	0.12	0.60	0.88
YU	0.76	0.05	0.71	0.83	0.74	0.05	0.68	0.79
EK	0.71	0.10	0.61	0.81	0.70	0.12	0.58	0.81
MR	0.70	0.10	0.59	0.82	0.67	0.09	0.55	0.77
UL	0.69	0.11	0.58	0.80	0.66	0.07	0.57	0.75
BA	0.54	0.05	0.49	0.58	0.55	0.08	0.47	0.62
ME	0.52	0.10	0.42	0.62	0.52	0.11	0.41	0.63
Overall	0.77	0.14	0.49	0.99	0.75	0.14	0.41	0.97

TABLE III
PARTICIPANTS PERFORMANCE IN 6-STATE BCI DISCRIMINATION TASK

Participant	Performance SVM				Performance LDA			
	Average	STD	Worst	Best	Average	STD	Worst	Best
ES	0.93	0.04	0.89	0.97	0.95	0.03	0.91	0.97
YL	0.87	0.03	0.84	0.89	0.90	0.02	0.88	0.92
HI	0.84	0.03	0.80	0.87	0.88	0.05	0.82	0.93
ER	0.79	0.09	0.70	0.86	0.84	0.08	0.76	0.89
EM	0.74	0.06	0.69	0.80	0.78	0.06	0.73	0.83
EK	0.63	0.11	0.52	0.74	0.73	0.09	0.64	0.82
YU	0.62	0.06	0.55	0.70	0.72	0.06	0.66	0.80
SE	0.60	0.07	0.50	0.66	0.67	0.09	0.55	0.75
UL	0.56	0.09	0.47	0.64	0.65	0.10	0.55	0.75
MR	0.49	0.10	0.37	0.61	0.56	0.15	0.38	0.74
ME	0.35	0.13	0.22	0.47	0.37	0.13	0.24	0.50
BA	0.33	0.04	0.29	0.37	0.33	0.05	0.29	0.38
Overall	0.64	0.19	0.29	0.97	0.70	0.19	0.29	0.99

III. RESULTS

A. Discrimination of Different Mental Imageries in Offline EEG BCI

We have determined performance of participants in 2-state (left and right hand movement imageries), 3-state (left and right hand movement imageries and passive mental imagery) and 6-state (left and right hand, left and right leg, tongue movement imageries, and passive imagery) BCI discrimination tasks via SVM and LDA-based decoders using FTA Cartesian features, and listed them in Table I, Table II and Table III respectively. In addition, standard deviations (STD) have been given in these tables. All accuracies reported are on per-trial basis. We have observed in all experiments that both SVM and LDA-based decoders using FTA Cartesian features showed similar results, with SVM showing a marginally better performance, on average outperforming LDA by 3–5% for all experiments.

It can be seen from Tables I, II and III that, we have grouped participants into high-performing, intermediate-performing and low-performing groups depending on their performance. The performance of high-performing group were stable across the experiments. This can be seen by analyzing participants' worst and best performance columns, which are the best and the worst performances among all distinct experiments of each participant.

The performance of the low-performing group is considered to be not satisfactory in the context of the end-goals of this work, which are the development of a model for a more generally useful BCI control of a robotic manipulator. Specifically, for more general usability of such a BCI, we consider the rate of BCI classification errors as satisfactory if it allows completion of robotic arm movements on average in $2\times$ or less the minimal necessary number of steps (that is, at 100% control accuracy).

In all experiments, we observed that the mental imagery states could be inferred from the EEG data with accuracy significantly above chance. However, the error rates significantly affect the use of EEG BCI communication paradigm for practical purposes. Specifically, the participants in high performing group were able to demonstrate 75–90% accuracy in 6-state BCI task, as compared to the baseline or "chance" performance of only 17%. These individuals' performance is far above chance and may be interesting for further investigation. At the same time, the performance of the other individuals in 6-state BCI task degraded significantly to 50–60% accuracy. While still significantly above chance, such rate of errors presents a serious obstacle on the way of utilizing this EEG BCI communication paradigm for practical purposes.

On the other hand, it is well known that left and right leg movements locations are really near each other on motor cortex therefore it is difficult to discriminate these movements. Despite this difficulty, it is observed in our experiments that left and right leg mental states are discriminated. Several examples of the average ERP curves in some specific EEG channels, showing that left and right leg mental states can be discriminated have been given in Fig. S3.

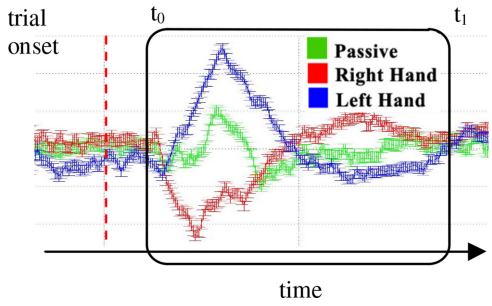

Fig. 4. Illustration of the trial onset-locked decoding data frame used to detect different mental imagery states in the EEG BCI signal.

B. Optimization of BCI Decoder

In this section, we consider several optimizations of BCI decoder parameters and design choices.

We first consider the optimization of the decoder's data frame selection. In order to detect different mental imagery states in EEG BCI data, a trial onset-locked data frames, $[t_0, t_1]$, are used for decoding as illustrated in Fig. 4.

Selection of the parameters of such data frames is important for optimizing the discrimination ability of the BCI decoder. In particular, making the decoding frame too large can obscure the relevant features due to accumulation of irrelevant noise contributed by uninformative EEG signal fragments immediately prior and immediately thereafter the useful EEG BCI signal. Likewise, choosing the data frame that is too small can miss such relevant signal all together.

To select the best such data frame parameters, we scanned over all possible choices of the initial frame offset, t_0, in the range from -0.5 sec to $+1.0$ sec (relative to trial onset signal) at a 0.1 sec increment. Likewise, we inspected different possible decoding data frame-length values, $dt = t_1 - t_0$, in the range between 0.2 and 2.0 sec, again at a 0.1 sec increments. We performed a complete search on the grid of such points for best parameters for each participant and each experiment. Fig. 5 shows the examples of the 2-state BCI discrimination accuracies for one high-performing individual (HI), one intermediately performing individual (YU), and one low-performing individual (BA). Several features can be pointed out in that figure. First, at the top-left corner of the diagrams a region with chance performance of just about 50% is observed. Upon closer examination, this region corresponds to the data frames such that lie entirely prior to the trial onset time. As the information about the mental imagery cannot possibly be contained in the decoding frames lying entirely prior to the trial onset signal, the decoder performance in that part of the diagram is at the simple chance level.

The decoder's performance increases sharply once the decoding frame begins to overlap with the region past the trial onset time at approximately 300–500 milliseconds. Indeed, the highest accuracy is consistently observed in the triangular region of the diagram defined by the frame initial offset t_0 of -0.5 to 0.3 sec and the frame length 0.2 to 0.9 sec. A rapid drop in performance is observed when t_0 exceeds 0.5 sec limit. This indicates that the information related to the identification

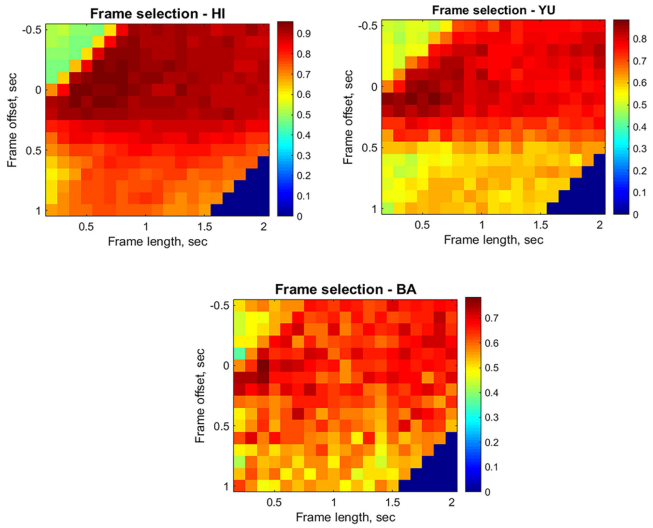

Fig. 5. Diagrams showing the accuracy of 2-state BCI discrimination versus the parameters of the decoder's data frame selection for one high-performing individual (HI), one intermediately performing individual (YU), and one low-performing individual (BA).

of mental imagery state is not present in the EEG signal after approximately 500 milliseconds past trial's onset signal.

Finally, we observe similar structure of the $t_0 - dt$ diagrams in Fig. 5 for each participant, whereas the lower-performing individuals only exhibit a lower increase in decoder's accuracy in the above mentioned best-detection triangle but otherwise the structure of the diagram remains the same.

All participants demonstrate close to optimal performance near the choice of the decoding frame parameters $t_0 = 0$–0.2 sec and $dt = 0.6$–0.9 sec. Thus, it appears possible to adopt a uniform choice of the decoding frame parameters $[t_0, t_1] = [0, 0.85]$ sec as a generally suitable for most participants, although fine-tuning of the decoding frame's position can allow moderate increase in BCI decoder's performance on individual experiment basis.

We second consider the issue of selecting the feature representation of EEG signal. The selection of feature representation of EEG signal for BCI decoder can significantly affect the BCI's performance. We investigate this effect here by examine the performance of BCI decoders built using EEG band power features, power spectral density (PSD) features, as well as new Fourier transform amplitude features. For all the signal power-based features such as EEG band powers and PSD, we inspect the row power and the log10 (that is, the Decibel) representation of such features. The row time-series (TS) features are likewise considered in this section: The time-series features had been used in EEG BCI in some past works, but did not find widespread use in EEG BCI literature. The above features' definitions have been briefly recapped in the supplementary material.

We test the performance of LDA and SVM-based BCI decoders using all of the above described feature sets for the purpose of optimizing our EEG BCI decoder, Table IV. While we observe that performance remains well above chance for all the above choices of EEG signal representation, FTA-Cartesian

TABLE IV
PERFORMANCE OF DIFFERENT FEATURE REPRESENTATIONS FOR MENTAL IMAGERY STATE DISCRIMINATION TASK

		EEG bands	log-EEG bands	PSD	log-PSD	FTA Polar	FTA Cartesian	Time series
SVM-2	Performance	0.770	0.769	0.780	0.766	0.812	0.910	0.897
	STD	0.099	0.087	0.088	0.090	0.103	0.099	0.098
SVM-3	Performance	0.579	0.594	0.580	0.560	0.624	0.744	0.757
	STD	0.114	0.105	0.098	0.106	0.112	0.140	0.139
SVM-6	Performance	0.439	0.427	0.422	0.384	0.432	0.594	0.597
	STD	0.126	0.119	0.113	0.133	0.132	0.194	0.192
LDA-2	Performance	0.698	0.710	0.740	0.717	0.769	0.860	0.858
	STD	0.092	0.082	0.074	0.089	0.090	0.102	0.101
LDA-3	Performance	0.578	0.612	0.586	0.563	0.622	0.754	0.734
	STD	0.140	0.107	0.100	0.118	0.114	0.137	0.123
LDA-6	Performance	0.443	0.439	0.453	0.415	0.493	0.646	0.605
	STD	0.150	0.280	0.125	0.156	0.155	0.211	0.183

TABLE V
THE IMPACT OF DIFFERENT CHOICES OF VOLTAGE REFERENCE ON THE BCI STATES DISCRIMINATION ACCURACY

		System 0V	Ground	Common	Laplace
EEG bands	Impact	0.727	0.770	0.760	0.748
	STD	0.063	0.650	0.061	0.073
log-EEG bands	Impact	0.713	0.748	0.769	0.762
	STD	0.061	0.069	0.060	0.064
PSD	Impact	0.719	0.768	0.779	0.761
	STD	0.061	0.063	0.065	0.067
log-PSD	Impact	0.697	0.748	0.766	0.752
	STD	0.057	0.067	0.063	0.068
FTA radial	Impact	0.782	0.803	0.800	0.812
	STD	0.073	0.065	0.065	0.063
FTA Cartesian	Impact	0.884	0.907	0.905	0.910
	STD	0.063	0.059	0.062	0.041
Time Series	Impact	0.874	0.897	0.892	0.893
	STD	0.068	0.059	0.055	0.065

features perform dramatically better than all of the other feature sets including EEG band power, PSD, and FTA-polar.

Since FTA-Cartesian features are a simple linear transformation of the EEG time-series, we can expect that the linear machine learning classifiers such as SVM and LDA will produce comparable performance on these feature sets. Indeed, we observe that in our experiments: both FTA-Cartesian and TS features provide similar performance for discrimination of up to 6 mental imagery states. However, as we will see below, FTA features have the added advantage of a more concise representation of the EEG signal with respect to frequency decomposition, which allows for a far smaller subset of FTA features to be used in the EEG BCI decoder without sacrificing the performance. While the SVM and LDA classifiers constructed in either time or frequency domain representations of the EEG signal can be mathematically shown to be equivalent, the equivalent time-domain BCI decoder constructed for, for example, a low-pass filtered EEG signal on frequency range [0, Fc] still requires multiplying and summing all the time samples x_t from the entire decoding window, whereas an BCI decoder constructed in frequency domain requires using only a small number of Fourier transform (FT) amplitudes in [0, Fc], in order to evaluate. This allows dramatically reducing computational costs of evaluating such frequency domain BCI decoders, which are especially important for such decoders being deployed in real-time settings. Therefore, we conclude that FTA-Cartesian features are the better choice for our EEG BCI.

Finally, we consider the issue of the referencing of the EEG data. When EEG data is acquired by an EEG acquisition device, it is recorded with respect to a particular voltage reference [21]. Choosing a different voltage reference affects the final representation of the EEG signal by adding or subtracting a time-varying common mode component. We inspect the impact of different choices of such referencing mode on the performance of EEG BCI decoders. Specifically, we examine the choices including the system's 0 Volt reference (in the Nihon Kohden EEG-1200 system), A1–A2 average reference (defined as the average of the voltages on A1 and A2 electrodes), the common reference (defined as the average potential of all EEG electrodes), and the Laplace reference (defined as the average of 4 neighbor electrodes for each electrode). The results of this analysis are presented in Table V.

Overall, we observe that the choice of reference voltage can have a noticeable impact on the EEG BCI performance for EEG band powers and PSD features. A BCI state detection accuracy improves up to 5% consistently when such references are used versus the system 0 Volt. In the case of FTA-Cartesian and TS features, the differences that can be attributed to the change of voltage reference are much less pronounced, with Laplace reference showing marginally better results.

C. The Information Content of EEG Signal by Frequency Range

Preprocessing of EEG signal by using low-pass filters is a common practice in EEG BCI [21]–[25]. In this work, we also observed that applying a low-pass filter to EEG signal can improve the performance of BCI decoder. In the case of the frequency-space features such as PSD or FTA, such a filtering can be implemented simply by rejecting those features that not fall into the pass-range [0, F_c]. In the case of TS features, we apply low-pass filter using 8th-order Butterworth low-pass filter. In either case, the effect of discarding high frequencies from EEG signal is found to be advantageous for the performance of EEG BCI. In fact, our experimentation suggests that keeping only the lowest frequency ranges of 0 to 5–10 Hz can result in the best overall performance of EEG BCI. The above experimentation suggests that most of useful BCI information in EEG signal is contained at very low frequencies. To investigate this issue further, we performed a series of numerical experiments in which the BCI decoder was constrained to use only the EEG data coming from a narrow 5 Hz-wide band, chosen in the frequency range 0–80 Hz.

In other words, we first inspected the BCI decoder using only the EEG data filtered to the frequency range of 0–5 Hz. Second, we inspected the BCI decoder using the EEG data filtered in the frequency band 5–10 Hz, 10–15 Hz and so on. We considered the EEG BCI decoders for 2, 3, and 6 mental state discrimination. In all cases, we observed that the ability of EEG BCI decoders to discriminate mental imageries degraded dramatically as the higher-frequency bands were selected, reducing to essentially the chance level after the threshold of approximately 20 Hz, Fig. 6. We conclude that the information relevant to the task of discriminating different motor imageries in an EEG BCI resides

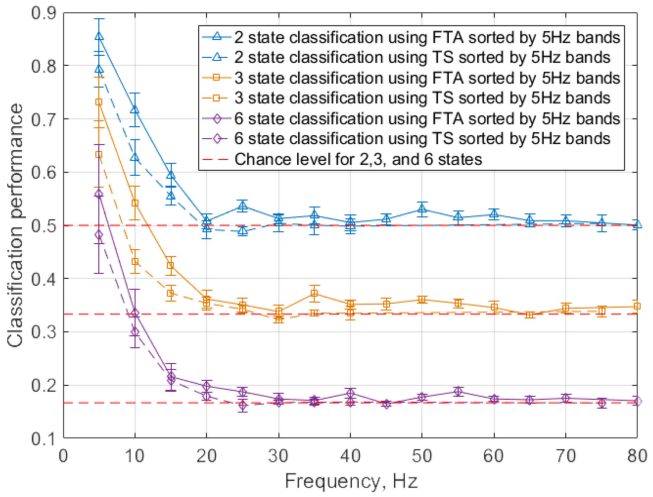

Fig. 6. The performance of EEG BCI decoder constrained to use narrow 5 Hz frequency bands in the range 0–80 Hz.

primarily in the low frequency range of 0–15 Hz, with the most such information residing in the range 0–5 Hz.

It is commonly known that the alpha/mu brain signals (8–13 Hz also known as sensorimotor rhythms) have been used to control motor movements in EEG based BCI [26]–[28]. However, not only sensorimotor rhythms but also low frequency (0–5 Hz) shifts in the EEG signal (slow potentials) such as movement related cortical potentials (MRCP) can be used for controlling motor movements too [24], [29]–[33]. (Several examples of the average ERP curves showing that salient responses associated with motor imageries occur on 200–600 ms (or 1–5 Hz) have been given in Fig. S2.) Unlike SMR-based BCIs that require longer training periods, slow potentials such as MRCP-based BCIs require much shorter training [30].

D. Consistency of BCI Performance Across Participants

In our experiments, we observe that the same participants tended to perform better in all experiments and for all types of BCI tasks, while the other same participants always tended to perform worse in all experiments. Table VI illustrates this observation by pulling together the performance data of different participants over all inspected BCI tasks and all experiments. As can be seen in Table VI, the top performing individuals perform better in all BCI tasks and all experiments. Likewise, the intermediate-level individuals performed at an intermediate level in all tasks, while the low-performing individuals always showed low levels of performance.

E. Online EEG BCI Applications

Our offline experiments indicated that both control strategies in principle could provide a similar average information throughput rate. However, we found in practice that substantially higher error rate of the 6-state control model proved to be frustrating for BCI users. Specifically, in our experiments the detection of the 3 mental imageries employed in the 3-state control model could be performed on average with 80–90% accuracy (see Results). At the same time, the detection of 6 mental imageries employed in the 6-state control model could be done with 50–60% accuracy. While these indicate that either 3- or 6-state control model provide similar information throughput of 1.2–1.5 bit per trial (0.4–0.5 bps), in practice, experiencing 1 in 2 error rate while attempting to control the 6-state BCI proved extremely frustrating and demotivating for the participants, negatively affecting their performance and resolve to master the control of the BCI. For this reasons we focused on the 3-state BCI control model in our online experiments.

We implemented an online, interactive EEG BCI system based on the hardware and the software described in the previous sections. The implemented system contained a virtual 3 dof-robot manipulator simulated in 3D on computer screen and capable of lateral motion, longitudinal motions, and hold-and-release motion. The manipulator could be controlled interactively by users by means of the EEG BCI, Fig. 7.

Three best performing individuals were invited to participate in the interactive BCI trials. Firstly, these individuals were asked to complete the training and practice sessions as described in Section II-B2 by using 3-state BCI control model.

Finally, in the test session the participants were given a series of task to move manipulator to different positions and attempted to complete them. The tasks included moving the manipulator in two (left-right or forward-backward) to four (left-right and forward-backward) directions for up to 4 steps. The participants completed in total 7–8 tasks during the 15-minute test sessions.

TABLE VI
CONSISTENCY OF BCI PERFORMANCE OF DIFFERENT INDIVIDUALS ACROSS BCI TASKS, ORDERED BY THE PARTICIPANTS' OVERALL PERFORMANCE LEVEL

Rank	Participant	2-state		3-state		6-state	
		Average	STD	Average	STD	Average	STD
1	ES	0.99	0.01	0.98	0.02	0.93	0.04
2	YL	0.98	0.01	0.90	0.01	0.87	0.03
3	HI	0.98	0.01	0.89	0.04	0.84	0.03
4	ER	0.95	0.06	0.89	0.06	0.79	0.09
5	EM	0.96	0.04	0.85	0.05	0.74	0.06
6	SE	0.95	0.05	0.82	0.12	0.60	0.07
7	YU	0.91	0.07	0.76	0.05	0.62	0.06
8	EK	0.84	0.09	0.71	0.10	0.63	0.11
9	MR	0.88	0.08	0.70	0.10	0.49	0.10
10	UL	0.81	0.05	0.69	0.11	0.56	0.09
11	ME	0.75	0.12	0.52	0.10	0.35	0.13
12	BA	0.77	0.02	0.54	0.05	0.33	0.04

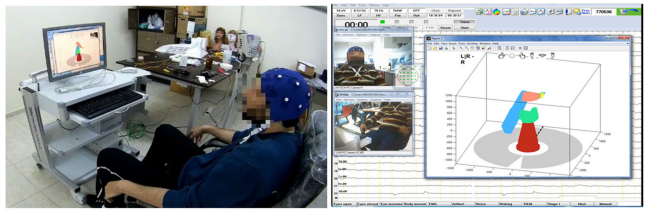

Fig. 7. Online experiments in which the participants have controled a 3 dof-robot manipulator arm using EEG BCI.

TABLE VII
PARTICIPANTS' PERFORMANCE IN ONLINE BCI EXPERIMENTS

Subject	HI	ER	ES
Tasks completed	100%	100%	40%
Accuracy	84.6%	77.6%	49.6%
Baseline time per sep	4.1 sec	4.1 sec	4.1 sec
Time per step	6.5 sec	9.3 sec	26.7 sec

The participants' performance was evaluated as the percentage of the tasks completed successfully, the average time taken to complete a task, and the average accuracy of the control of the manipulator. The control accuracy was quantified as the percentage of the manipulator moves that were in correct directions moving the manipulator towards the target. The best participant (HI) had shown in the interactive trials the average control accuracy of 84.6%, and the second best participant (ER) had shown in the interactive trials the control accuracy of 77.8%, which was consistent with the results observed for these participants in the segment of this work's analyses performed offline. The third participant (ES) experienced greater difficulties controlling the BCI, being able to control the BCI with an average accuracy of only 49.6%, far below the performance levels shown in the offline experiments. The successful participants required 7 to 10 seconds to implement one manipulator move, on average. The participant HI spent 6.5 seconds and the participant ER required 9.3 seconds to implement each manipulator's move. Due to the BCI control model here, the BCI could accept on average one command per a 3 second period, equal to the time per one "on"-signal's presentation in the BCI. Together with the time necessary for switching the regime of motion of the BCI, this implied on average 4.1 seconds per manipulator move – the best-case scenario. The best participant, therefore, was able to control the manipulator with 50% time overhead and 15% error rate, while the second best participant required approximately twice the ideal amount of time and made close to 25% errors controlling the BCI. Due to difficulty controlling the BCI that the third participant experienced, that participant spent from 13 to 40 seconds per move in successful trials, being able to complete only 40% of assigned tests. The other two subjects were able to complete 100% of the tasks given to them. The results of interactive BCI application are summarized in Table VII.

IV. DISCUSSION

In our experiments, we distinguish as many as 6 mental imagery states in EEG BCI well above chance level. In our offline experiments, the group-average BCI performances have been found as 90% for two tasks, 77% for three tasks, and 64% for six tasks. These results are consistent and in many cases superior to similar results reported in the literature [34]–[39].

We study the impact of different choices in the design of EEG BCI decoder parameters on BCI performance, including the choice of EEG signal's feature representation, the choice of decoder's detection frame parameters, the choice of voltage reference, and other choices. We observe that FTA features show superior performance outperforming by close to 30% all of the features based on calculating the EEG signal power spectrum, such as used in the EEG BCI literature conventionally. In this work, the EEG signal power features are shown to achieve up to 78% discrimination accuracy on 2-state BCI discrimination task, average over all participants, whereas FTA features allow the same discrimination to be performed with greater than 90% accuracy. For discrimination of 6 mental imageries, the EEG signal power features allow up to 45% discrimination accuracy, while the use of FTA features results in 65% accuracy on average over all participants and up to 85–90% for best individuals. The use of FTA features in this work, therefore, allows achieving a significant improvement in the performance of EEG BCI.

Low-pass filtering of EEG signal prior to its processing in BCI is a common practice in EEG BCI literature. We also observe that low-pass filtering can help improve the performance of the decoder in the EEG BCI. Furthermore, we observe that low-pass filtering the EEG signal to only 5 Hz high-cutoff results in some of the best performance of the BCI. This suggests that most useful information about the motor-based mental imagery used in this work resides at very low frequencies in the EEG signal.

Indeed, similar results – that the useful information in EEG BCI may be encoded by the lowest EEG frequency bands – is also indicated in past studies including such of upper limb movement intentions [24], [40], [41], studies involving field potential [42]–[44], ECoG [45]–[47], and closed-loop studies with implanted intra-cortical electrodes [48]. On the other hand, traditionally motor-imagery EEG BCI have used power modulation in higher frequency bands of EEG signal such as mu (8–13 Hz) and beta (20–30 Hz) rhythms [26]–[28].

We inspect this situation in greater depth by testing the discriminability of mental motor imageries using the EEG data filtered to different narrow 5 Hz-bands ranging from 0–5 Hz to 75–80 Hz. We observe that the ability of EEG BCI to distinguish such motor imagery states drops rapidly as the frequency of the EEG filtering band increases past 15–20 Hz. Only 0–5 Hz, 5–10 Hz and 10–15 Hz frequency bands allow the EEG BCI performance that is significantly different from chance, and only the frequencies of 0–5 Hz and 5–10 Hz show such performance better than the chance by a meaningful margin. Specifically, in the case of discriminating the motor imageries of left and right hand movements, the all-participants average discrimination accuracy observed using the EEG signal in 0–5 Hz band in our experiments was 80–90%, for 5–10 Hz–65–75%, and for 10–15 Hz–55–60% - just slightly above the chance level of 50%. Beyond 15 Hz, the discrimination accuracy for this BCI task was not different from chance. At the same time, for discriminating 6 mental imagery states, the all-participants average accuracy was 50–60% when using 0–5 Hz frequency band, 30–35% when using 5–10 Hz band, and 20–23% for 10–15 Hz band, with the higher bands again showing no difference from the chance level of 16%. We conclude that the low frequencies of 0–15 Hz carry the most significant information related to the different motor imageries used in EEG BCI, with most of such information coming from the frequency band of only 0–10 Hz.

In our study, the participants demonstrated consistent performance when grouped into high-performing, intermediate-performing and low-performing groups. 5 out of 12 participants

demonstrated high level of performance using our BCI, achieving in the offline experiments the accuracy on 2-state BCI task of 95–100%, 3-state BCI task of 85–90%, and 6-state BCI task of 80–90%. These individuals demonstrated high performance related to all BCI tasks and consistently in all experiments. In online BCI trials, these participants showed good ability to control the BCI in interactive settings demonstrating the ability to execute motions using a simulated 3D robotic manipulator arm and the BCI with 80% accuracy at a rate of 6–9 moves per minute. The ability of these individuals to control the BCI presents interest for further practical application. 5 out of 12 participants demonstrated intermediate levels of performance achieving the accuracy of 80–90% in 2-state BCI task, 70–80% in 3-state BCI task, and 50–70% in 6-state BCI task. 2 out of 12 participants could not achieve a satisfactory BCI control ability, in the context of the end-goals of this work which are the development of a model for a more generally useful BCI control of a robotic manipulator. While these individuals still showed performance significantly above chance while using our BCI, they could achieve the BCI control accuracy of only 75% in 2-state scenario, 50% in 3-state scenario, and 35% in 6-state scenario.

In our online experiments, a single 15-minute session was used for training the BCI decoder. This was done because the participants' intent during the practice and the test sessions deemed to not be reliably known, given the design choices made in our experiments. In principle, such design can be seen as suboptimal, whereas suggestions for decoder learning involving also the practice and the test sessions have been made in the literature [49], [50]. One common approach for that can be to treat the BCI moves consistent with the target pursued by the user in a test or practice session as correct. On the other hand, other studies have suggested that learning BCI can be viewed as a process similar to learning the use of any other tool [12]. Thus, the process of BCI application can be structured intentionally in such a way that a moderately successful BCI decoder is offered to the users first, and then the users adapt to the decoder, which happens by changing of the users' neural patterns in the brain, to better grasp the control of the fixed BCI. In this scenario, the BCI decoder needs to remain fixed intentionally, in order to assist the user in that adaptation process [3]. Distinguishing among these two possibilities is one of the future targets for our work.

In EEG BCI, high session-to-session variability of the EEG signal and accompanying need for re-training the BCI is well known [51]–[53]. While the reasons for that variability are not well understood, they may include session-to-session variability in electrode placement, changes in scalp and electrode impedance due to humidity, temperature, channel motion, sweat, as well as emotional, hormonal, and pharmacological changes. Similarly, in our experiments we observe the need for retraining or re-calibrating the BCI decoder in each experiment. The necessity to train the decoder for each new application of the BCI is a disadvantage of existing EEG BCI technology. However, in this work the training session lasted for only 15 minutes, and after that the same decoder was used until the end of the experiment. This training time is much shorter than that described in other BCI studies [54]–[57].

V. Conclusions

In this work, we study the possibility of implementing an EEG-based BCI for high-performance control of an assistive robot manipulator in 3 dimensions. For this purpose, we carry out an extensive offline study of mental imagery discrimination using EEG BCI as well as perform online BCI control experiments. We use motor imagery BCI control paradigm successful in the literature and inspect different design choices of such an EEG BCI. Our results indicate that the levels of performance interesting for practical applications can be achieved using EEG BCI with only noninvasive neural activity imaging modality. In our experiments, best individuals demonstrated up to 80–90% control accuracy with up to 6 BCI states in offline settings, and 80–90% control accuracy using 3 mental imagery states in interactive, online settings. However, our 6-state online BCI experiments have not been successful for now. We are still working to develop more fruitful designing approaches for 6-state online BCI experiments.

On the other hand, we observe in our study that a group of several individuals demonstrated consistently high BCI performance, while a group of other individuals was not able to achieve satisfactory performance at all. This observation is consistent with the notion of "BCI literacy" in modern EEG BCI literature [58]–[60]. Certain inherent, either psychological or physiological parameters may be responsible for this variability in the ability of different individuals to control EEG BCI. If so, focusing on the design of EEG BCI tailored to specific individuals with the ability to control them may be a plausible strategy for the development of practically applicable EEG BCI.

References

[1] M. A. Lebedev and M. A. L. Nicolelis, "Brain-machine interfaces: Past, present and future," *Trends Neurosci.*, vol. 29, no. 9, pp. 536–546, 2006.
[2] B. He *et al.*, "Brain–Computer Interfaces," in *Neural Engineering*. Boston, MA, USA: Springer, 2013, pp. 87–151.
[3] J. M. Carmena *et al.*, "Learning to control a brain-machine interface for reaching and grasping by primates," *PLoS Biol.*, vol. 1, no. 2, pp. 193–208, 2003.
[4] M. Velliste *et al.*, "Cortical control of a prosthetic arm for self-feeding," *Nature*, vol. 453, pp. 1098–1101, 2008.
[5] S. T. Clanton *et al.*, "Seven degree of freedom cortical control of a robotic arm," in *Brain-Computer Interface Research: A State-of-the-Art Summary*. Berlin, Germany: Springer, 2013, pp. 73–81.
[6] G. Schalk *et al.*, "Two-dimensional movement control using electrocorticographic signals in humans," *J. Neural Eng.*, vol. 5, no. 1, pp. 75–84, 2008.
[7] K. Ganguly and J. M. Carmena, "Emergence of a stable cortical map for neuroprosthetic control," *PLoS Biol.*, vol. 7, no. 7, 2009, Art. no. e1000153.
[8] L. R. Hochberg *et al.*, "Neuronal ensemble control of prosthetic devices by a human with tetraplegia," *Nature*, vol. 442, no. 7099, pp. 164–171, 2006.
[9] L. R. Hochberg *et al.*, "Reach and grasp by people with tetraplegia using a neurally controlled robotic arm," *Nature*, vol. 485, no. 7398, pp. 372–375, 2012.
[10] J. L. Collinger *et al.*, "High-performance neuroprosthetic control by an individual with tetraplegia," *Lancet*, vol. 381, no. 9866, pp. 557–564, 2013.
[11] S. Waldert *et al.*, "A review on directional information in neural signals for brain-machine interfaces," *J. Physiol. Paris*, vol. 103, nos. 3–5, pp. 244–254, 2009.
[12] T. J. Bradberry *et al.*, "Fast attainment of computer cursor control with noninvasively acquired brain signals," *J. Neural Eng.*, vol. 8, no. 3, 2011, Art. no. 036010.

[13] D. J. McFarland *et al.*, "Electroencephalographic (EEG) control of three-dimensional movement," *J. Neural Eng.*, vol. 7, no. 3, 2010, Art. no. 036007.

[14] J. R. Wolpaw and D. J. McFarland, "Control of a two-dimensional movement signal by a noninvasive brain-computer interface in humans," *Proc. Nat. Acad. Sci. USA*, vol. 101, no. 51, pp. 17849–17854, 2004.

[15] J. R. Wolpaw *et al.*, "An EEG-based brain-computer interface for cursor control," *Electroencephalography Clin. Neurophysiol.*, vol. 78, no. 3, pp. 252–259, 1991.

[16] A. S. Royer *et al.*, "EEG control of a virtual helicopter in 3-dimensional space using intelligent control strategies," *IEEE Trans. Neural Syst. Rehabil. Eng.*, vol. 18, no. 6, pp. 581–589, Dec. 2010.

[17] T. Carlson and J. Del R. Millan, "Brain-controlled wheelchairs: A robotic architecture," *IEEE Robot. Autom. Mag.*, vol. 20, no. 1, pp. 65–73, Mar. 2013.

[18] J. Meng *et al.*, "Noninvasive electroencephalogram based control of a robotic arm for reach and grasp tasks," *Sci. Rep.*, vol. 6, no. 1, 2016, Art. no. 38565.

[19] K. LaFleur *et al.*, "Quadcopter control in three-dimensional space using a noninvasive motor imagery-based brain–computer interface," *J. Neural Eng.*, vol. 10, no. 4, 2013, Art. no. 046003.

[20] F. Lotte *et al.*, "A review of classification algorithms for EEG-based brain-computer interfaces," *J. Neural Eng.*, vol. 4, no. 2, pp. R1–R13, 2007.

[21] M. Teplan, "Fundamentals of EEG measurement," *Meas. Sci. Rev.*, vol. 2, no. 2, pp. 1–11, 2002.

[22] C. Vidaurre *et al.*, "Time domain parameters as a feature for EEG-based brain-computer interfaces," *Neural Netw.*, vol. 22, no. 9, pp. 1313–1319, 2009.

[23] R. Tomioka and K. R. Müller, "A regularized discriminative framework for EEG analysis with application to brain-computer interface," *Neuroimage*, vol. 49, no. 1, pp. 415–432, 2010.

[24] B. Blankertz *et al.*, "Classifying single trial EEG: Towards brain computer interfacing," *Adv. Neural Inf. Process. Syst.*, vol. 1, pp. 157–164, 2002.

[25] Y. Wang *et al.*, "BCI Competition 2003 - Data set IV: An algorithm based on CSSD and FDA for classifying single-trial EEG," *IEEE Trans. Biomed. Eng.*, vol. 51, no. 6, pp. 1081–1086, Jun. 2004.

[26] B. He *et al.*, "Noninvasive brain-computer interfaces based on sensorimotor rhythms," *Proc. IEEE*, vol. 103, no. 6, pp. 907–925, Jun. 2015.

[27] G. Pfurtscheller and F. H. Lopes, "Event-related EEG/MEG synchronization and desynchronization: basic principles," *Clin. Neurophysiol.*, vol. 110, pp. 1842–1857, 1999.

[28] H. Yuan *et al.*, "Cortical imaging of event-related (de)Synchronization during online control of brain-computer interface using minimum-norm estimates in frequency domain," *IEEE Trans. Neural Syst. Rehabil. Eng.*, vol. 16, no. 5, pp. 425–431, Oct. 2008.

[29] I. K. Niazi *et al.*, "Detection of movement intention from single-trial movement-related cortical potentials," *J. Neural Eng.*, vol. 8, no. 6, Oct. 2011, Art. no. 066009.

[30] I. K. Niazi *et al.*, "Detection of movement-related cortical potentials based on subject-independent training," *Med. Biol. Eng. Comput.*, vol. 51, no. 5, pp. 507–512, May 2013.

[31] F. Karimi *et al.*, "Detection of movement related cortical potentials from EEG using constrained ICA for brain-computer interface applications," *Front. Neurosci.*, vol. 11, Jun. 2017, Art. no. 356.

[32] J. N. Spring *et al.*, "Movement-related cortical potential amplitude reduction after cycling exercise relates to the extent of neuromuscular fatigue," *Front. Human Neurosci.*, vol. 10, Jun. 2016, Art. no. 257.

[33] R. Xu *et al.*, "Factors of influence on the performance of a short-latency non-invasive brain switch: Evidence in healthy individuals and implication for motor function rehabilitation," *Front. Neurosci.*, vol. 9, Jan. 2016, Art. no. 527.

[34] J. Müller-Gerking *et al.*, "Designing optimal spatial filters for single-trial EEG classification in a movement task," *Clin. Neurophysiol.*, vol. 110, no. 5, pp. 787–798, 1999.

[35] B. Obermaier *et al.*, "Information transfer rate in a five-classes brain-computer interface," *IEEE Trans. Neural Syst. Rehabil. Eng.*, vol. 9, no. 3, pp. 283–288, Sep. 2001.

[36] E. Gysels and P. Celka, "Phase synchronization for the recognition of mental tasks in a brain-computer interface," *IEEE Trans. Neural Syst. Rehabil. Eng.*, vol. 12, no. 4, pp. 406–415, Dec. 2004.

[37] C. Jeunet *et al.*, "Predicting mental imagery-based BCI performance from personality, cognitive profile and neurophysiological patterns," *PLoS One*, vol. 10, no. 12, pp. 1–21, 2015.

[38] E. Abdalsalam *et al.*, "Classification of four class motor imagery for brain computer interface," in *Proc. 9th Int. Conf. Robot, Vis., Signal Process. Power Appl.*, 2017, pp. 297–305.

[39] G. Onose *et al.*, "On the feasibility of using motor imagery EEG-based brain – computer interface in chronic tetraplegics for assistive robotic arm control: A clinical test and long-term post-trial follow-up," vol. 50, pp. 599–608, 2012.

[40] T. J. Bradberry *et al.*, "Reconstructing three-dimensional hand movements from noninvasive electroencephalographic signals," *J. Neurosci.*, vol. 30, no. 9, pp. 3432–3437, 2010.

[41] A. Y. Paek *et al.*, "Decoding repetitive finger movements with brain activity acquired via non-invasive electroencephalography," *Front. Neuroeng.*, vol. 7, 2014, Art. no. 3.

[42] A. K. Bansal *et al.*, "Relationships among low-frequency local field potentials, spiking activity, and three-dimensional reach and grasp kinematics in primary motor and ventral premotor cortices," *J. Neurophysiol.*, vol. 105, no. 4, pp. 1603–1619, 2011.

[43] T. M. Hall *et al.*, "A common structure underlies low-frequency cortical dynamics in movement, sleep, and sedation," *Neuron*, vol. 83, no. 5, pp. 1185–1199, 2014.

[44] M. Mollazadeh *et al.*, "Spatiotemporal variation of multiple neurophysiological signals in the primary motor cortex during dexterous reach-to-grasp movements," *J. Neurosci.*, vol. 31, no. 43, pp. 15531–15543, 2011.

[45] S. Acharya *et al.*, "Electrocorticographic amplitude predicts finger positions during slow grasping motions of the hand," *J. Neural Eng.*, vol. 7, no. 4, Aug. 2010, Art. no. 046002.

[46] T. Pistohl *et al.*, "Decoding natural grasp types from human ECoG," *Neuroimage*, vol. 59, no. 1, pp. 248–260, 2012.

[47] J. Kubánek *et al.*, "Decoding flexion of individual fingers using electrocorticographic signals in humans," *J. Neural Eng.*, vol. 6, no. 6, Dec. 2009, Art. no. 066001.

[48] J. A. Perge *et al.*, "Reliability of directional information in unsorted spikes and local field potentials recorded in human motor cortex," *J. Neural Eng.*, vol. 11, no. 4, Aug. 2014, Art. no. 046007.

[49] J. DiGiovanna *et al.*, "Coadaptive brain - machine interface via reinforcement learning," *IEEE Trans. Biomed. Eng.*, vol. 56, no. 1, pp. 54–64, Jan. 2009.

[50] A. L. Orsborn *et al.*, "Closed-loop decoder adaptation on intermediate time-scales facilitates rapid BMI performance improvements independent of decoder initialization conditions," *IEEE Trans. Neural Syst. Rehabil. Eng.*, vol. 20, no. 4, pp. 468–477, Jul. 2012.

[51] P. S. Hammon and V. R. De Sa, "Preprocessing and meta-classification for brain-computer interfaces," *IEEE Trans. Biomed. Eng.*, vol. 54, no. 3, pp. 518–525, Mar. 2007.

[52] J. Faller *et al.*, "A co-adaptive brain-computer interface for end users with severe motor impairment," *PLoS One*, vol. 9, no. 7, pp. 1–10, 2014.

[53] E. Cinar and F. Sahin, "New classification techniques for electroencephalogram (EEG) signals and a real-time EEG control of a robot," *Neural Comput. Appl.*, vol. 22, no. 1, pp. 29–39, Jan. 2013.

[54] B. Blankertz *et al.*, "The Berlin brain–computer interface: EEG-based communication without subject training," *IEEE Trans. Neural Syst. Rehabil. Eng.*, vol. 14, no. 2, pp. 147–152, Jun. 2006.

[55] E. Buch *et al.*, "Think to move: A neuromagnetic brain-computer interface (BCI) system for chronic stroke," *Stroke*, vol. 39, no. 3, pp. 910–917, 2008.

[56] C. Guger *et al.*, "Real-time EEG analysis with subject-specific spatial patterns for a brain-computer interface (BCI)," *IEEE Trans. Rehabil. Eng.*, vol. 8, no. 4, pp. 447–456, Dec. 2000.

[57] M. Thulasidas *et al.*, "Robust classification of EEG signal for brain-computer interface," *IEEE Trans. Neural Syst. Rehabil. Eng.*, vol. 14, no. 1, pp. 24–29, Mar. 2006.

[58] M. Ahn *et al.*, "High theta and low alpha powers may be indicative of BCI-illiteracy in motor imagery," *PLoS One*, vol. 8, no. 11, 2013, Art. no. e80886.

[59] F. Gembler *et al.*, "Autonomous parameter adjustment for SSVEP-based BCIs with a novel BCI wizard," *Front. Neurosci.*, vol. 9, pp. 1–12, 2015.

[60] Y. U. Khan and F. Sepulveda, "Wrist movement discrimination in single-trial EEG for brain computer interface using band powers," *Int. J. Biomed. Eng. Technol.*, vol. 6, no. 3, pp. 272–285, 2011.